IDA-PBC under sampling for torque control of PMSM

M. Khanchoul * **M. Hilairet** **, **D. Normand-Cyrot** ***

* *LGEP/SPEE Labs; CNRS UMR8507; SUPELEC; Univ Pierre et Marie Curie-P6; Univ Paris Sud-P11, 91192 Gif sur Yvette, France*
** *Franche-Comté Electronique Mécanique Thermique et Optique - Sciences et Technologies" (FEMTO-ST), Université de Franche-Comté, Belfort, France*
*** *L2S; CNRS UMR 8506; SUPELEC; Université Paris-Sud 11, 91192 Gif sur Yvette*
Email: mohamed.khanchoul@lgep.supelec.fr, mickael.hilairet@univ-fcomte.fr, cyrot@lss.supelec.fr

Abstract: A nonlinear passivity-based control can be suitably used to achieve stability of a permanent magnet synchronous machine (PMSM). Nevertheless, passivity properties are usually lost when such a controller is implemented in a sampled-data context and, as a consequence, stabilization objectives are degraded. This paper proposes a direct sampled-data control strategy based on the IDA-PBC techniques, in order to keep the same performances with a higher sampling period. Therefore, this type of controller is able to be implemented in a low-performance DSP.

Keywords: Permanent magnet synchronous motor (PMSM), port-controlled Hamiltonian systems, IDA-PBC, direct sampled-data IDA-PBC.

1. INTRODUCTION

Nowadays, PMSM are used in many fields. This gain in popularity is due to his attractive features such as: high power/mass ratio, rapid dynamic response due to high torque-to-inertia ratio, high efficiency, compactness, and simple modeling and control [Bose, 2002]. In addition, the presence of the magnet in the rotor reduced the Joule losses due to the absence of winding excitation in the rotor that makes PMSM highly efficient.

Several stable position and velocity controllers for PMSM have been reported in the control literature, such as the field oriented control (FOC) and the direct torque control (DTC)[Buja and Kazmierkowski, 2004, Wang et al., 2007]. These controllers can be designed using a cascade of two controllers, for instance, an outer loop for the speed control and inner loops for the currents control. These controllers are based on PI or IP controllers, adaptive PI controller [Li and Liu, 2009], sliding mode controller [Baik et al., 2002, Laghrouche et al., 2004], predictive controller [Mariethoz et al., 2009], backstepping controller [Zhou and Wang, 2002], Lyapunov-based controller [Hernandez-Guzman and Silva-Ortigoza, 2011] or passivity-based controller [Petrovic et al., 2001, Akrad et al., 2007]. The recently developed energy-shaping technique [Ortega and Garcia-Canseco, 2004, Ortega et al., 2008] or interconnection and damping assignment passivity-based control (IDA-PBC), has been applied to design new globally stable controllers for PMSMs [Akrad et al., 2007]. In a practical context, integral action are added in order to improve the robustness. A technique that preserves the Halmiltonian form and closed-loop stabiliy with integral action on the passive outputs is presented in [Donaire and Junco, 2009, Donaire et al., 2012] and is applied to PMSM speed control. Nevertheless, in a practical way, when the controller is implemented by a computer, the system is placed in a sampled-data context and, as it is well known, passivity properties are usually lost [Monaco et al., 2008]. Consequently, passivity based controllers (PBC) implemented through a zero order holder device (emulation process) lose their validity. In practice, the designers choose a sampling period so that the response time is at least equal to 20 times the sampling period or opt for very small controller gain value.

In this paper, a direct sampled-data IDA-PBC strategy is proposed to control the currents of a permanent synchronous motor with a regular field oriented control strategy. This work is based on a recent theory [Tiefensee et al., 2010, Monaco et al., 2011] called digital passivity based control. An analysis on the performances according to the sampling frequency is discussed. Finally, the computational cost of this new controller is compared with the usual implementation through emulation of a continuous-time IDA-PBC strategy.

This paper is organized as follows: In section II, the regular IDA-PBC method is recalled and applied to the currents control of a PMSM. The sampled-data passivity based control strategy is detailed in section III. Finally, simulations and discussions are treated in section IV.

2. THE CONTINUOUS-TIME IDA-PBC APPROACH

In continuous time, the fundamental idea of IDA-PBC is to shape a desired internal structure and then to dissipate the energy of the whole system through damping injection. Interconnection and damping assignment passivity-based control is a technique that shapes the behavior of nonlinear systems assigning a desired port-controlled Hamiltonian (PCH) structure to the closed-loop.

2.1 Recalls about the theory

The procedure starts with the system's description in the port controlled Hamiltonian structure:

$$\begin{aligned} \dot{x} &= [\mathcal{J}(x) - \mathcal{R}(x)]\nabla H(x) + g(x)u + \zeta \\ y &= g^T \nabla H(x) \end{aligned} \tag{1}$$

where $x \in \mathbb{R}^n$ is the state vector, $u \in \mathbb{R}^m$ is the control vector, $y \in \mathbb{R}^m$ is the output vector with $m < n$, ζ a perturbation, $H : \mathbb{R}^n \longrightarrow \mathbb{R}$ is the total stored energy, $\mathcal{J}(x) = -\mathcal{J}(x)^T$, $\mathcal{R}(x) = \mathcal{R}^T(x) \geq 0$ are the interconnection and damping matrices respectively. PCH model have been selected by the fact that they are natural candidates to describe many physical systems.

Proposition 1 : Consider the nonlinear system [Ortega and Garcia-Canseco, 2004]

$$\dot{x} = f(x) + g(x)u \tag{2}$$

assume there are matrices $g^\perp(x)$, $\mathcal{J}_d(x) = -\mathcal{J}_d^T(x)$, $\mathcal{R}_d(x) = \mathcal{R}_d^T(x) \geq 0$ and a function $H_d(x) : \mathbb{R}^n \longrightarrow \mathbb{R}$ that verify the partial differential equation (PDE)

$$g^\perp(x)f(x) = g^\perp(x)[\mathcal{J}_d(x) - \mathcal{R}_d(x)]\nabla H_d \tag{3}$$

where $g^\perp(x)$ is a full-rank left annihilator of $g(x)$, that is, $g^\perp(x)g(x) = 0$, and $H_d(x)$ is such that

$$x^* = argmin(H_d(x)) \tag{4}$$

with $x^* \in \mathbb{R}^n$ the (locally) equilibrium point to be stabilized. Then, the closed-loop system (2) with the control u, where

$$\begin{aligned} u &= \left[g^T(x)g(x)\right]^{-1} g^T(x) \\ &\times \left\{[\mathcal{J}_d(x) - \mathcal{R}_d(x)]\nabla H_d - f(x)\right\} \end{aligned} \tag{5}$$

takes the PCH form

$$\dot{x} = [\mathcal{J}_d(x) - \mathcal{R}_d(x)]\nabla H_d \tag{6}$$

Stability of x^* is established noting that, along the trajectories of (6), we have

$$\dot{H}_d = -\left[\nabla H_d\right]^T \mathcal{R}_d(x)\nabla H_d \leq 0 \tag{7}$$

Hence, $H_d(x) \geq 0$ qualifies as a Lyapunov function. It will be asymptotically stable if, in addition, x^* is an isolated minimum of $H_d(x)$ and also the unique solution of the (8) :

$$\left\{x \in \mathbb{R}^n | \left[\nabla H_d\right]^T \mathcal{R}_d(x)\nabla H_d = 0\right\} \tag{8}$$

Asymptotic stability follows immediately invoking the La Salle's invariance principle.

2.2 Permanent Magnet Synchronous Motor Control via IDA-PBC

The model of the synchronous machine is defined in the (dq) coordinates as follows:

$$\begin{aligned} L_d\frac{di_d}{dt} &= -R_s i_d + P\Omega L_q i_q + v_d \\ L_q\frac{di_q}{dt} &= -R_s i_q - P\Omega(L_d i_d + \phi) + v_q \\ J\frac{d\Omega}{dt} &= P\left(L_d - L_q\right) i_d i_q + P\phi i_q - f\Omega - \tau_l \end{aligned} \tag{9}$$

In these equations, P is the number of pole pairs, v_d, v_q, i_d, i_q are the voltages and the currents in the (dq) coordinate, L_d and L_q are the stator inductances which are equal for surface Permanent-Magnet Machinesin (PMSM), R_s is the stator winding resistance, τ_l is an unknown load torque, f is the friction coefficient, ϕ and J are the flux produced by the permanent magnets and the moment of inertia respectively and Ω the mechanical speed. The PCH model of the PMSM takes the form (2) with

$$g = \begin{bmatrix} 1 & 0 \\ 0 & 1 \\ 0 & 0 \end{bmatrix} \quad u = \begin{bmatrix} v_d \\ v_q \end{bmatrix} \quad \zeta = \begin{bmatrix} 0 \\ 0 \\ -\tau_l \end{bmatrix}$$

$$\mathcal{J}(x) = \begin{bmatrix} 0 & 0 & Px_2 \\ 0 & 0 & -P(x_1 + \phi) \\ -Px_2 & P(x_1 + \phi) & 0 \end{bmatrix}$$

$$\mathcal{R}(x) = \begin{bmatrix} R_s & 0 & 0 \\ 0 & R_s & 0 \\ 0 & 0 & f \end{bmatrix}, \quad x = \begin{bmatrix} L_d i_d \\ L_q i_q \\ J\Omega \end{bmatrix}$$

The desired equilibrium state for synchronous machines is usually selected based on the so called "maximum torque per ampere" principle as: $x^* = [0, (L_q\tau_l/P\phi), J\Omega^*]^T$. The design procedure proposed in the latter paragraph leads to the continuous-time linear controller [Akrad et al., 2007]:

$$u = \begin{bmatrix} (R_s - r_1)i_d - PL_d i_q^*\Omega + P(L_d - L_q)i_q\Omega^* \\ (R_s - r_2)i_q + r_2 i_q^* + P\phi\Omega^* \end{bmatrix} \tag{10}$$

where r_1 and r_2 are strictly positive gains. Therefore, the closed loop plant can be written as:

$$\dot{\tilde{x}} = [\mathcal{J}_d - \mathcal{R}_d]\nabla H_d \tag{11}$$

where $\tilde{x} = x - x^*$ and $\mathcal{J}_d(x) - \mathcal{R}_d$ equal to:

$$\mathcal{J}_d(x) - \mathcal{R}_d = \begin{bmatrix} -r_1 & PL_d\Omega & \left(L_d - L_q\right) i_q \\ -PL_d\Omega & -r_2 & -\phi \\ -\left(L_d - L_q\right) i_q & \phi & 0 \end{bmatrix}$$

The system storage function H_d is

$$H_d\left(\tilde{x}\right) = \frac{1}{2}\tilde{x}^T Q\, \tilde{x}, \quad \text{with} \quad \mathrm{Q} = \begin{bmatrix} \frac{1}{L_d} & 0 & 0 \\ 0 & \frac{1}{L_q} & 0 \\ 0 & 0 & \frac{P}{J} \end{bmatrix} \tag{12}$$

where the minimum is reached at the point of equilibrium x^*.

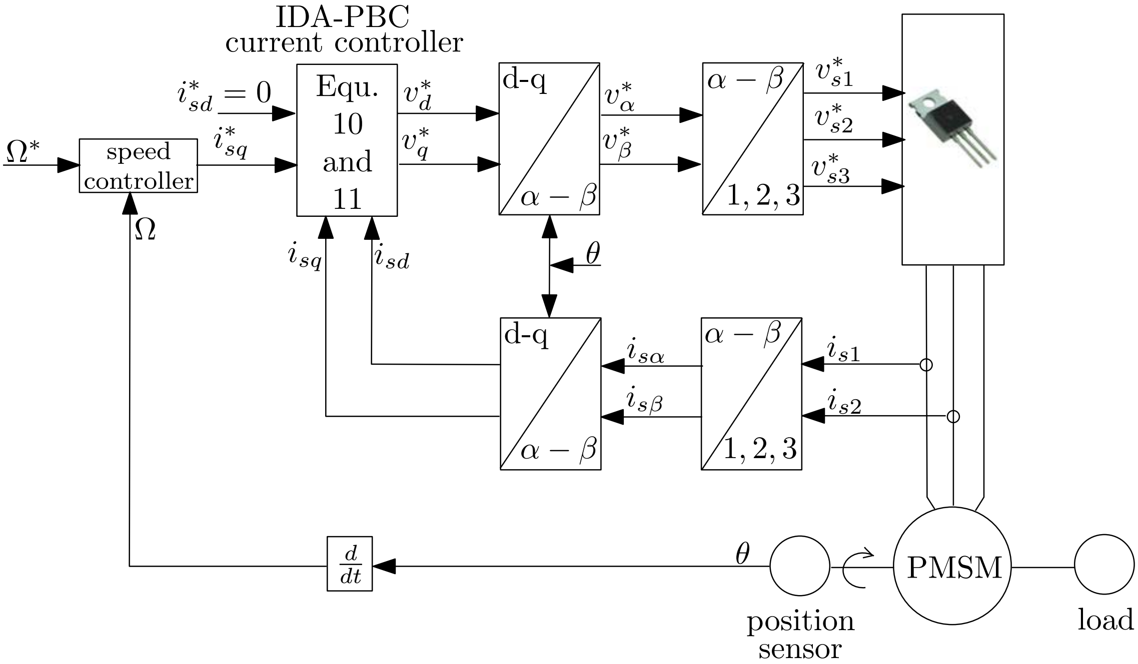

Fig. 1. IDA-PBC structure with a RST speed controller.

Finally, the design of the speed controller is based on a digital linear controller as shown on Fig. 1 and gives the desired q-axis current i^*_{sq}.

Remark 1: Tuning of r_1 **and** r_2 In practice, the tuning of the degree of freedom of nonlinear controller is not easily as for linear system. Here, if the measured speed is nearly equal to the desired speed, the controller compensates the back-emf of the machine and the transfert functions of the closed-loop currents d and q can be represented by first order functions, i.e. $H(p) = \frac{1}{1+\tau\, p}$ with $\tau = L_d/r_1$ or L_q/r_2. It immediately follow that the time response of the closed-loop d or q-axis currents are $t_{rd} = \frac{3\, L_d}{r_1}$ or $t_{rq} = \frac{3\, Lq}{r_2}$ and easily tune.

3. SAMPLED-DATA IDA-PBC DESIGN

In this section, a new digital controller is developed. The main objective is to ensure the stabilization at the equilibrium point x^* with a good transient response under large sampling periods.

In this paragraph, the closed-loop continuous-time state is denoted by x_c and continuous-time control by u_c. The sampled-data state under a piecewise controller u_k is denoted, at the time-instants $t = kT_e$ by x_k, its value at the instant $t = (k+1)T_e$ is denoted by x_{k+1}. In this sense, if there exists a piecewise controller u_k under which the energetic behavior of u_c is matched at the sampling instants then, the equality below must be verified for all x_k such that $x_c(t = kT_e) = x_k$:

$$H_d(x_{k+1}) - H_d(x_k) = \int_{kT_e}^{(k+1)T_e} \dot{H}_d(x_c(\tau))d\tau \tag{13}$$

The left hand side of (13) represents the desired energetic evolution of the sampled-data system and can be computed as follows:

$$H_d(x_{k+1}) - H_d(x_k) = \frac{1}{2}\left(e^{T_e((\mathcal{J}-\mathcal{R})Qx+g(.)u_k)} - I_d\right)(x_k - \bar{x})^T Q (x_k - \bar{x}) \tag{14}$$

where $e^f(.) := 1 + \sum_{i\geq 1} \frac{\mathrm{L}_f^i}{i!}$, is the Lie series operator associated with a given vector field f, I_d the identity operator and $\mathrm{L}_f(.) = \sum_{i=1}^n f_i(.)\frac{\partial}{\partial x_i}$ denotes the Lie derivative operator associated with a given vector field f on R^n (see [Monaco and Normand-Cyrot, 1997] for more details). The right hand size of (13) represents the energetic evolution of x_c and can be exactly computed as:

$$\begin{aligned}&\int_{kT_e}^{(k+1)T_e} \dot{H}_d(x_c(\tau))\mathrm{d}\tau \\ &= H_d(x_c|_{t=(k+1)T_e}) - H_d(x_c|_{t=kT_e}) \\ &= x_k^T\left(\left(e^{T_e(\mathcal{J}-\mathcal{R})Q}\right)^T Q e^{T_e(\mathcal{J}_d-\mathcal{R}_d)Q} - Q\right)x_k\end{aligned}$$

The sampled-data controller u_k is described by its series expansion in T_e around the continuous-time one $u_{k0} = u_c|_{t=kT_e}$ as $u_k = u_{k0} + \sum_{i\geq 1} \frac{T_e}{(i+1)!}u_{ki}$, and each so-called "corrective" term u_{ki} is computed by comparing and equating homogeneous terms in powers of T_e in the equality (13). The computation of an exact solution being in general a difficult task due to the nonlinearities describing the continuous-time dynamics, an interesting solution can proposed at the first order of approximation, i.e.

$$u_k = u_{k0} + \frac{T_e}{2!}u_{k1} \tag{15}$$

with:

$$u_{k0} = u_c \tag{16}$$

$$u_{k1} = \dot{u}_c \tag{17}$$

It follows that the new control input u_k is:

$$u_k = [\text{ Eq. (10) }] + \frac{T_e}{2!}\begin{bmatrix} v_{d1} \\ v_{q1} \end{bmatrix} \tag{18}$$

with

$$\begin{aligned} v_{d1} = & \frac{R_s - r_1}{L_d}\big(- r_1 i_d + P\Omega(L_q i_q - L_d i_q^*) \\ & + P(L_d - L_q) i_q \Omega^*\big) - \frac{P^2}{J} L_d i_q i_q^* \big((L_d - L_q) i_d + \Phi\big) \\ & + \big(\frac{P}{L_q} L_d \Omega^* - P\Omega^*\big)(-r_2(i_q - i_q^*) \\ & - P\Phi(\Omega - \Omega^*) - P L_d i_d \Omega) \end{aligned} \tag{19}$$

$$\begin{aligned} v_{q1} = & \frac{R_s - r_2}{L_q}\big(- r_2(i_q - i_q^*) - P\phi(\Omega - \Omega^*) \\ & - P L_d i_d \Omega\big) \end{aligned} \tag{20}$$

In the case of a non-salient rotor ($L_d = L_q = L$), the previous equations become:

$$\begin{aligned} v_{d1} = & \frac{R_s - r_1}{L}(-r_1 i_d + P L i_q \Omega - P L i_q^* \Omega) \\ & - \frac{P^2}{J} L i_q^* \phi i_q \end{aligned} \tag{21}$$

$$\begin{aligned} v_{q1} = & \frac{R_s - r_2}{L}(-r_2(i_q - i_q^*) - P L i_d \Omega \\ & - P\phi(\Omega - \Omega^*)) \end{aligned} \tag{22}$$

Remark 2: Numerous systems are described by a first order model, i.e. $H(p) = \frac{1}{Ap+B}$ that leads to the continuous passivity controller:

$$u_0 = Bx^* + (B - R_d)(x - x^*), \quad \text{with} \quad \mathrm{R_d} \geq 0 \tag{23}$$

The corrective terms u_n are connected by the following recurrence relation:

$$\begin{aligned} u_1 &= -\frac{B - R_d}{A}(x - x^*) \\ u_n &= -\frac{R_d}{A} u_{n-1}, \quad \text{for} \quad \mathrm{n} \geq 2 \end{aligned} \tag{24}$$

leading to a simple, few time-consuming computation and performing controller.

4. SIMULATION AND DISCUSSIONS

To control the speed of the PMSM, a RST controller ensure this function and the IDA-PBC control the (dq) currents, as shown on Fig. 1. In order to highlight the performances of the new digital controller, a comparison between the latter, emulated controller based on the continuous-time design and the continuous controller are detailed for different sampled periods.

Firstly, three control laws are compared for two configurations: a) closed-loop dynamique equal to 2 ms and a sample time T_e equal to 1 ms, b) closed-loop dynamique equal to 0.2 ms and a sample time T_e equal to 0.1 ms.

Figs. 2.a-2.b show the step response of current i_q controlled at zero speed by the continuous IDA-PBC, emulated IDA-PBC (implementation of the continuous IDA-PBC with a zero-order holder, Eq. 10), sampled IDA-PBC (Eq. 18). i_{qc}, i_{qe} and i_{qk} represent the currents controlled by the continuous IDA-PBC, the emulated IDA-PBC and sampled IDA-PBC respectevely. The simulation shows that the current i_{qe} doesn't reproduce the trajectory of the current i_{qc} with the adopted tuning. Moreover, this latter is under-damping compared with i_{qk} in configuration b (see Fig. 2.b). Fig. 2.c show that the sampled-data controlled reproduce exactly the continuous IDA-PBC current whit increasement of the expansion order.

Figs. 3-4 show the mechanical speed and the quadrature current i_q which is control by the continuous IDA-PBC, emulated IDA-PBC or the sample-data IDA-PBC. The simulation shows that the three current controllers have the same behavior with a sampling period equal to 100μs.

It is interesting to note that currents i_{qc} and i_{qk} are in advance compared to the desired currents while the measured speed doesn't reached the desired value. It means that the right part of Equ. 10 introduce a "feedforward" term in the controller.

Secondly, the sampled period has been increased gradually. Figs. 5-6 show that for a sampling time equal to $T_e = 3$ ms, the emulated IDA-PBC strategy fail, while the other one keeps a good performances. It confirms the effectiveness of this new controller in a sampled-date context.

While sampled-data controller still ensures a good current regulation, with acceptable ripple, the emulated strategy degrades the control objectives. Moreover, the shape of the current which is controlled by the sampled-data IDA-PBC remains smooth. The simulation shows that current ripples begin to appear when the sampling period is greater than 4 ms with the emulated IDA-PBC. It important to note that the maximum sampling-time given in this work depend of the machine and the closed-loop dynamic (tuning of r_1 and r_2).

Finally, the computational cost of this new controllers are compared to the regular emulated IDA-PBC, as shown in Tab. 1. We can notice that the ratio “number of operations/sampling period” of the two controllers is lower for the sampled-data controller for the same system performances. Moreover, the use of higher sampling period with the new controller reduces the number of push/pop operations of the stack to save or restore the registers (computer science).

Table 1. Algorithm complexity

	Emulated controller		Sample-data controller	
	Number of additions and sous-traction	Number of multi-plications	Number of additions and sous-traction	Number of multi-plications
Non salient machine	3	5	12	18
Salient machine	4	6	18	29

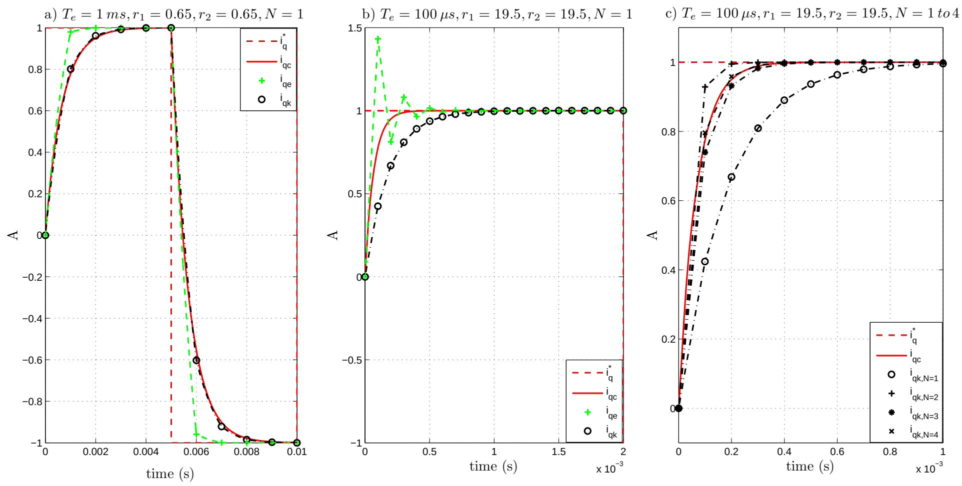

Fig. 2. Current response for different tuning.

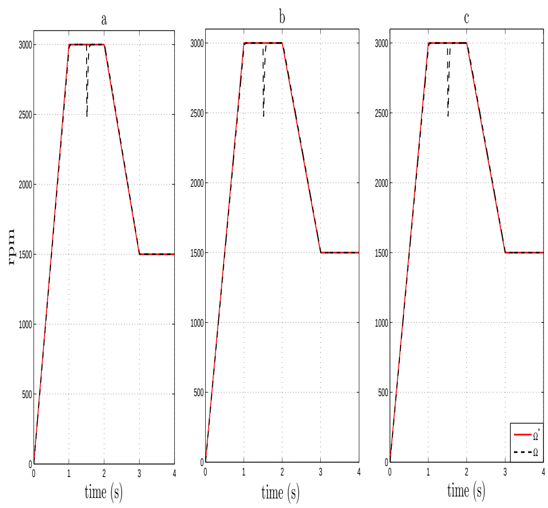

Fig. 3. Desired and measured speed - (a) continuous controller, (b) emulated controller, (c) sample-data controller $(N = 1)$ - $T_e = 100\,\mu s, r_1 = 0.65, r_2 = 0.65$

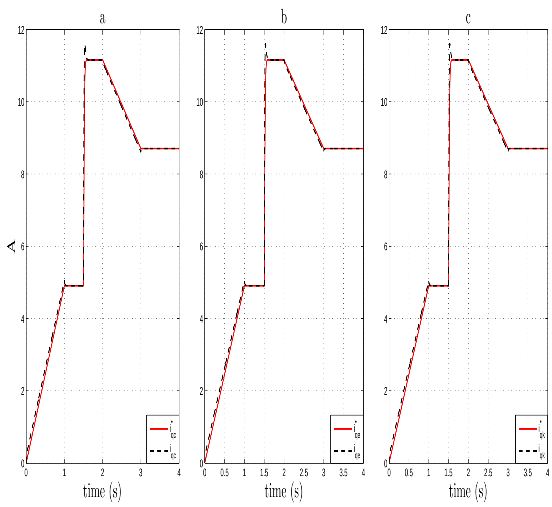

Fig. 4. Desired and measured q-axis current - (a) continuous controller, (b) emulated controller, (c) sample-data controller $(N = 1)$ - $T_e = 100\,\mu s, r_1 = 0.65, r_2 = 0.65$

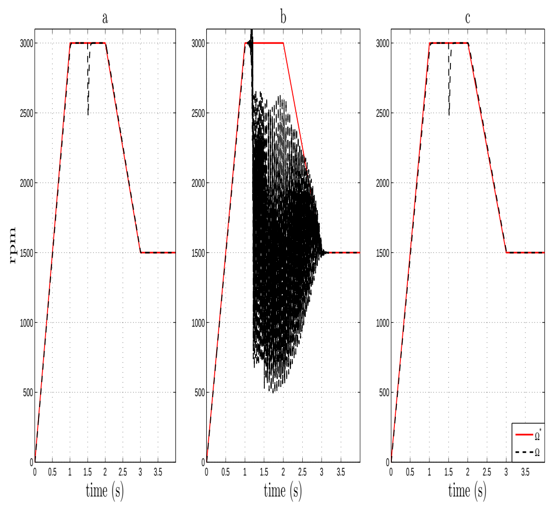

Fig. 5. Desired and measured speed - (a) continuous controller, (b) emulated controller, (c) sample-data controller $(N = 1)$ - $T_e = 3\,\mathrm{ms}, \mathrm{r}_1 = 0.65, \mathrm{r}_2 = 0.65$

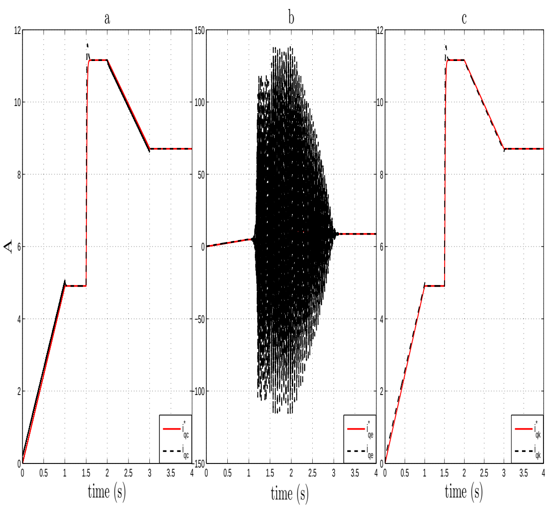

Fig. 6. Desired and measured q-axis current - (a) continuous controller, (b) emulated controller, (c) sample-data controlle $(N = 1)$ - $T_e = 3\,\mathrm{ms}, \mathrm{r}_1 = 0.65, \mathrm{r}_2 = 0.65$

5. CONCLUSION

A direct sampled-data controller based on the IDA-PBC technique is developed for the current control of a PMSM. Such a controller is compared with the regular implementation, so-called emulated strategy, which consists to implement the continuous-time controller through a zero order holder device. The simulation shows that the performances of the emulated control decrease while the sampling period increase. On the contrary, the sampled-data IDA-PBC ensures a good current control although the high sampling time.

Acknowledgment: This research was supported by the PEPS project “GESE: Gestion Echantillonnée des Systèmes Energétiques”, 2010.

Table 2. Machine parameters

Rated output power	$P_n = 6\,\mathrm{kW}$
Rated torque	$C_n = 5.5\,\mathrm{N.m}$
Rated speed	$N = 6000\,\mathrm{rpm}$
Rated voltage	$V_n = 350\,\mathrm{V}$
Rated current	$I_n = 22.5\,\mathrm{A}$
Stator resistance	$R_s = 0.165\,\Omega$
Stator inductance d-axis	$L_d = 0.95\,\mathrm{mH}$
Stator inductance q-axis	$L_q = 1\,\mathrm{mH}$
Rated flux	$\Phi = 0.03\,\mathrm{Wb}$
Number of pole pairs	$P = 5$
Inertia load	$J = 6.10^{-4}\,\mathrm{Kg.m}^2$
Viscous coefficient	$f = 0,0005\,\mathrm{N.m/s}$

REFERENCES

A. Akrad, M. Hilairet, D. Diallo, and R. Ortega. Interconnection and damping assignment approach for reliable pm synchronous motor control. *IET Colloquium on Reliability in Electromagnetic Systems*, pages 1–6, May 2007.

I. Baik, K.H. Kim, and M-J Young. Robust nonlinear speed control of pm synchronous motor using boundary layer integral sliding mode control technique. *IEEE Transactions on Control Systems Technology*, 8(1):47–54, 2002.

B.K. Bose. *Modern power electronics and AC drives.* Prentice Hall, 2002.

G.S. Buja and M.P. Kazmierkowski. Direct torque control of pwm inverter-fed ac motors - a survey. *IEEE Transactions on Industrial Electronics*, 51(4):744–757, 2004.

A. Donaire and S. Junco. On the addition of integral action to port-controlled hamiltonian systems. *Automatica*, 45(8):1910–1916, 2009.

A. Donaire, T. Perez, and Y.R. Teo. Robust speed tracking control of synchronous motors using immersion and invariance. *7th IEEE Conference on Industrial Electronics and Applications (ICIEA)*, pages 1482–1487, July 2012.

V.M. Hernandez-Guzman and R. Silva-Ortigoza. Pi control plus electric current loops for pm synchronous motors. *IEEE Transactions on Control Systems Technology*, 19(4):868–873, 2011.

S. Laghrouche, F. Plestan, and A. Glumineau. A higher order sliding mode controller for a class of mimo nonlinear systems: application to pm synchronous motor control. *American Control Conference*, 3:2592–2597, 2004.

Shihua Li and Zhigang Liu. Adaptive speed control for permanent-magnet synchronous motor system with variations of load inertia. *IEEE Transactions on Industrial Electronics*, 56(8):3050–3059, 2009.

S. Mariethoz, A. Domahidi, and M. Morari. A model predictive control scheme with torque ripple mitigation for permanent magnet motors. *35th Annual Conference of IEEE Industrial Electronics IECON*, pages 2943–2948, 2009.

S. Monaco and D. Normand-Cyrot. On nonlinear digital control - nonlinear systems - control 3. *A.J. Fossard and D. Normand-Cyrot, Eds., Chapman & Hall*, pages 127–155, 1997.

S. Monaco, D. Normand-Cyrot, and F. Tiefensee. From passivity under sampling to a new discrete-time passivity concept. *Proc. 47th IEEE CDC*, pages 3157–3162, 2008.

S. Monaco, D. Normand-Cyrot, and F. Tiefensee. Sampled-data stabilization; a pbc approach. *IEEE Transactions on Automatic Control*, 56(4):907–912, 2011.

R. Ortega and E. Garcia-Canseco. Interconnection and damping assignment passivity-based control: A survey. *European Journal of Control*, 10:432–450, 2004.

R. Ortega, A. van der Schaft, F. Castanos, and A. Astolfi. Control by interconnection and standard passivity-based control of port-hamiltonian systems. *IEEE Transactions on Automatic Control*, 53(11):2527–2542, 2008.

V. Petrovic, R. Ortega, and A.M. Stankovic. Interconnection and damping assignment approach to control of pm synchronous motors. *IEEE Transactions on control*, 9 (6):811–819, 2001.

F. Tiefensee, S. Monaco, and D. Normand-Cyrot. Ida-pbc under sampling for port-controlled hamiltonian systems. *American Control Conference (ACC)*, pages 1811–1816, 2010.

Yi Wang, Jianguo Zhu, and Youguang Guo. A survey of direct torque control schemes for permanent magnet synchronous motor drives. *Power Engineering Conference AUPEC*, pages 1–5, Dec. 2007.

J. Zhou and Y. Wang. Adaptive backstepping speed controller design for a permanent magnet synchronous motor. *IEE Proceedings Electric Power Applications*, 149(2):165–172, 2002.